

Measurements and Monte Carlo calculation of radial dose and anisotropy functions of BEBIG ^{60}Co high-dose-rate brachytherapy source in a bounded water phantom

Buchapudi Rekha Reddy, MSc, Dip. R.P.¹, Marc J P Chamberland, PhD^{2,3}, Manickam Ravikumar, PhD⁴, Chandraraj Varatharaj, PhD^{1,3}

¹Department of Radiation Physics, Kidwai Memorial Institute of Oncology, Bangalore, India, ²Carleton Laboratory for Radiotherapy Physics, Department of Physics, Carleton University, Ottawa, Canada, ³Division of Medical Physics, The University of Vermont Medical Center, Burlington VT, USA, ⁴Department of Radiotherapy, Sri Shankara Cancer Hospital & Research Centre, Shankarapuram, Bangalore, India

Abstract

Purpose: The study compared the experimentally measured radial dose function, $g(r)$, and anisotropy function, $F(r,\theta)$, of a BEBIG ^{60}Co (Co0.A86) high-dose-rate (HDR) source in an in-house designed water phantom with egs_brachy Monte Carlo (MC) calculated values. MC results available in the literature were only for unbounded phantoms, and there are no currently published data in the literature for experimental data compared to MC calculations for a bounded phantom.

Material and methods: egs_brachy is a fast EGSnrc application designed for brachytherapy applications. For unbounded phantom calculation, we considered a cylindrical phantom with a length and diameter of 80 cm and used liquid water. These egs_brachy calculated TG43U1 parameters were compared with the consensus data. Upon its validation, we experimentally measured $g(r)$ and $F(r,\theta)$ in a precisely machined $30 \times 30 \times 30 \text{ cm}^3$ water phantom using TLD-100 and EBT2 Gafchromic Film and compared it with the egs_brachy results of the same geometry.

Results: The TG43U1 dosimetric dataset calculated using egs_brachy was compared with published data for an unbounded phantom, and found to be in good agreement within 2%. From our experimental results of $g(r)$ and $F(r,\theta)$, the observed variation with the egs_brachy code calculation is found to be within the acceptable experimental uncertainties of 3%.

Conclusions: In this study, we validated the egs_brachy calculation of the TG43U1 dataset for the BEBIG ^{60}Co source for an unbounded geometry. Subsequently, we measured the $g(r)$ and $F(r,\theta)$ for the same source using an in-house water phantom. In addition, we validated these experimental results with the values calculated using the egs_brachy MC code, with the same geometry and similar phantom material as used in the experimental methods.

J Contemp Brachytherapy 2019; 11, 6: 563–572

DOI: <https://doi.org/10.5114/jcb.2019.91224>

Key words: Monte Carlo code, radial dose function, anisotropy function.

Purpose

In brachytherapy, dosimetric challenges are difficult to overcome due to very steep dose gradients, small treatment distances, and the magnitude of variation of the dose deposited across the treatment volumes of interest. As per the joint recommendations of the American Association of Physicists in Medicine (AAPM) and the European Society for Therapeutic Radiology and Oncology (ESTRO) [1], all radiation sources used in high-dose-rate (HDR) brachytherapy practice must have a dosimetry

dataset with all relevant parameters available, based on the Task Group No. 43 update (TG43U1) formalism [2], and also provide the consensus data for photon-emitting brachytherapy sources with an average energy higher than 50 keV [3]. Since these data vary with the type of the source, as they are highly dependent on the size of the active core of the source, the isotope distribution, and the encapsulation material and its geometry, it is recommended that specific dosimetric data should be obtained by appropriate methods, either by experimental or Monte

Address for correspondence: Dr. Ravikumar Manickam, PhD, Professor of Radiation Physics, Department of Radiotherapy, Sri Shankara Cancer Hospital & Research Centre, Shankarapuram, Bangalore – 560004, India, phone: +91-80-26094043, fax: +91-80-26560723, e-mail: drmravi59@yahoo.com

Received: 11.07.2019

Accepted: 03.12.2019

Published: 23.12.2019

Carlo (MC) calculations, which may be used as inputs in the treatment planning system [4,5,6,7,8,9].

However, to the best of our knowledge, there are no data available in the literature that compare the measured radial dose function, $g(r)$, and the anisotropy function, $F(r,\theta)$, with the MC calculation of the BEBIG ^{60}Co (Co0.A86) source based on the TG43U1 formalism in a single study. Hence, the present study aimed to compare the measured $g(r)$ and $F(r,\theta)$ of the BEBIG ^{60}Co HDR source, using thermoluminescent dosimetry (LiF-TLD100) and Gafchromic EBT2 Film dosimetry in an in-house designed water phantom, with the egs_brachy MC calculated values in a similar geometry. As a prerequisite for this study, we validated the egs_brachy MC code for the BEBIG ^{60}Co source by calculating the dosimetric data set in accordance with the TG43U1 recommendations for an unbounded phantom and compared it with published literature data.

Material and methods

Monte Carlo calculation methods

egs_brachy MC Code

The egs_brachy application was used for Monte Carlo calculations. It is an EGSnrc application which uses the egs++ class library [10,11,12]. The publication by Chamberland *et al.* [13] provides a general overview of the egs_brachy application, a complete discussion of all features, details on benchmarking and characterization of simulation efficiency, and some sample calculation times for clinical scenarios.

Modelling of the BEBIG ^{60}Co HDR source

The BEBIG ^{60}Co HDR source (Co0.A86) consists of a pure cobalt ($\rho = 8.9 \text{ gm/cm}^3$) cylindrical core (diameter 0.05 cm, length 0.35 cm). Radioactive ^{60}Co is uniformly distributed inside this active core. The source core is encapsulated by steel (outer diameter 0.1 cm, inner diameter 0.07 cm). The capsule is 0.5 cm long and has a thickness of 0.075 cm along the long axis on the proximal end to the cable. There is an air gap of 0.01 cm around the axial side of the active core. A stainless steel cable with a length of 5 mm and a diameter of 0.9 mm is attached to the source. The geometric design and material details of the BEBIG

^{60}Co source (Co0.A86) are taken from a published study [9]. The schematic egs_brachy modelled source is shown in Figure 1.

egs_brachy MC calculation for unbounded phantom

To validate the egs_brachy MC calculation for the BEBIG ^{60}Co source, as mentioned above, we calculated the TG43U1 parameters, such as dose rate constant (Λ), $g(r)$, and $F(r,\theta)$ for an unbounded phantom and compared the results with the consensus data [3]. For these calculations, we considered a cylindrical phantom with a length and diameter of 80 cm and used liquid water with a density of 0.998 g cm^{-3} at 22°C , as recommended by TG43U1. The scoring region in the water phantom was divided into cylindrical shells for the varying voxel sizes to minimize its effect with dosimetric data. The sizes of the voxels were chosen as follows: $0.1 \text{ mm} \times 0.1 \text{ mm}$ voxels were used for the distance of $r \leq 1 \text{ cm}$, $0.5 \text{ mm} \times 0.5 \text{ mm}$ voxels for $1 < r \leq 5 \text{ cm}$, $1 \text{ mm} \times 1 \text{ mm}$ voxels for $5 < r \leq 10 \text{ cm}$, and $2 \text{ mm} \times 2 \text{ mm}$ voxels for $10 < r \leq 20 \text{ cm}$ to provide the adequate spatial resolution. The air kerma strength per history was obtained as $4.2350 \pm 0.0024 \times 10^{-13} \text{ Gy cm}^2/\text{history}$ using the approach of Taylor and Rogers [14,15]. To calculate the dose rate constant (Λ), we used the dose to water per history on the reference position ($1 \text{ cm}, \Pi/2$) in the unbounded water phantom, divided by the air kerma strength per history. The radial dose function, $g_L(r)$, calculated for an unbounded phantom, in this study, is denoted as $g(r)_{\text{unbou}}$. It was calculated from 0.2 cm to 20 cm using line source geometry functions ($L = 3.5 \text{ mm}$). We calculated the anisotropy functions, $F(r,\theta)$, for an unbounded phantom in this study, which is denoted as $F(r,\theta)_{\text{unbou}}$ using the line source approximation and tabulated at radii of 0.25, 0.5, 0.75, 1, 2, 3, 4, 5, 7.5, 10, 12.5, 15, and 20 cm for the polar angles from 0° to 180° with varying intervals. As per the recommendations of AAPM Task Group 268 on reporting Monte Carlo studies, Table 1 summarizes parameters of the Monte Carlo calculations [2,9,13,16,17,18,19].

Experimental methods

Thermoluminescent dosimeters (LiF TLD-100)

The TLD experiment was performed using a fresh batch of lithium fluoride doped with magnesium and

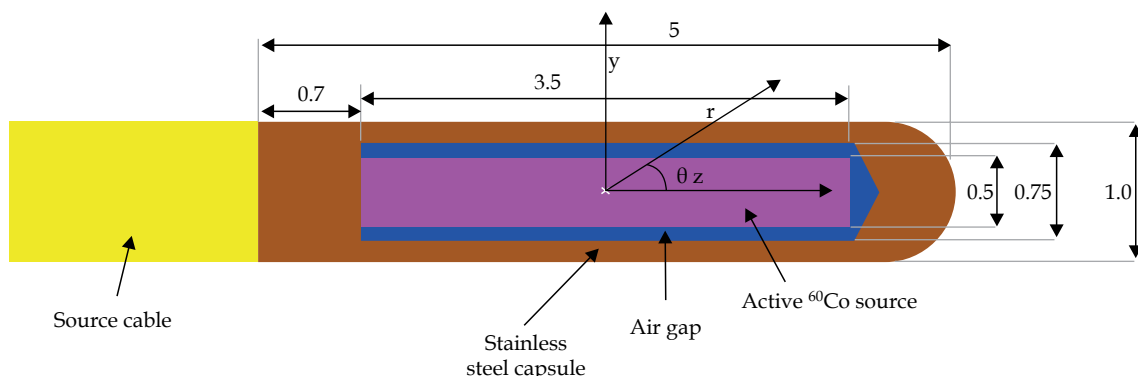


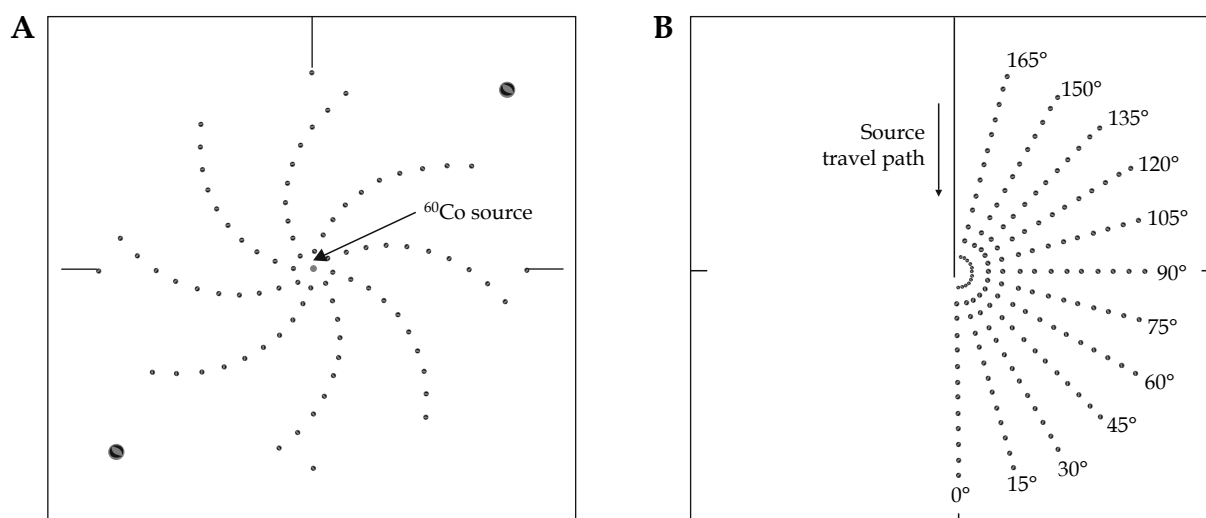
Fig. 1. Schematic diagram of the BEBIG ^{60}Co source modelled in egs_brachy with the egs++ class library (all dimensions in mm, but not to scale)

Table 1. Summary of the parameters used in the Monte Carlo calculations based on AAPM TG 286 report

Item name	Description	References
Code, version, release date	egs_brachy, pre-release version, Spring 2016; based on EGSnrc release 2016	[13]
Validation	Validation of the egs_brachy MC code	[13]
Timing	1,500-6,500 total CPU hours on Intel Xeon 5160 CPUs with clock speeds of 3.0 GHz	
Source description	Isotropic photon emission based on the photon part of the ^{60}Co spectrum. Contributions to the dose from the electron part of the spectrum are negligible due to the steel encapsulation. The photons are uniformly distributed in the cobalt core of the source ($\rho = 8.9 \text{ gm/cm}^3$ cylindrical core, diameter 0.05 cm, length 0.35 cm)	[9]
Cross-sections	Photon cross-sections from XCOM database. Atomic transitions from the Livermore Evaluated Atomic Data Library (EADL). Mass-energy absorption coefficients calculated using the EGSnrc application 'g'	[16,17]
Transport parameters	Photon cutoff energy (PCUT) = 1 keV Electron cutoff energy (ECUT) = 10 keV Interactions modelled: Rayleigh scattering bound Compton scattering, photoelectric absorption, fluorescent emission of characteristic x-rays, electron impact ionization. All other transport parameters use the default values from EGSnrc	[18]
VRT and AIET	Dose scoring used the tracklength estimator for situations where electronic equilibrium exists (e.g., > 1 cm away from the source)	[13]
Scored quantities	Dose to medium using either the tracklength estimator or interaction (energy deposition) scoring	[13]
# histories and statistical uncertainties	4e9 to 2e10 histories; sufficient to obtain 1 statistical uncertainties (type A) of 2% or less at a distance of 10 cm from the source	
Statistical methods	Uncertainties are calculated with the default history-by-history method used in EGSnrc	[19]
Post-processing	The calculated dose distributions were not filtered in any way. TG-43 parameters were calculated using the TG43U1 formalism	[2]

titanium (LiF: Mg, Ti) TLD-100 square rods with dimensions of $1 \times 1 \times 6 \text{ mm}^3$. Before each experiment, the TLDs were annealed according to the technique proposed by Booth *et al.* [20], known as "prereadout" annealing. The response of the TLD rods was analyzed using an automated Harshaw Biocron TLD reader (model 3500) and the annealing was carried out using the Thermolyne Furnace (model 47900). The integrated area under the

glow curve for a temperature of 270°C was evaluated to obtain the TL output in nC. The relative responses, termed elemental correction factors (ECF), were determined by irradiating the whole batch of TLD rods with a dose of 2 Gy in ^{60}Co γ -rays from the Theratron-780C telecobalt unit. The ECF were determined five times and the TLD rods that showed a variation greater than 2% (type A) were discarded. The individual calibration fac-

**Fig. 2.** Design of the precisely machined: (A) radial PMMA slab phantom and (B) anisotropy PMMA slab phantom

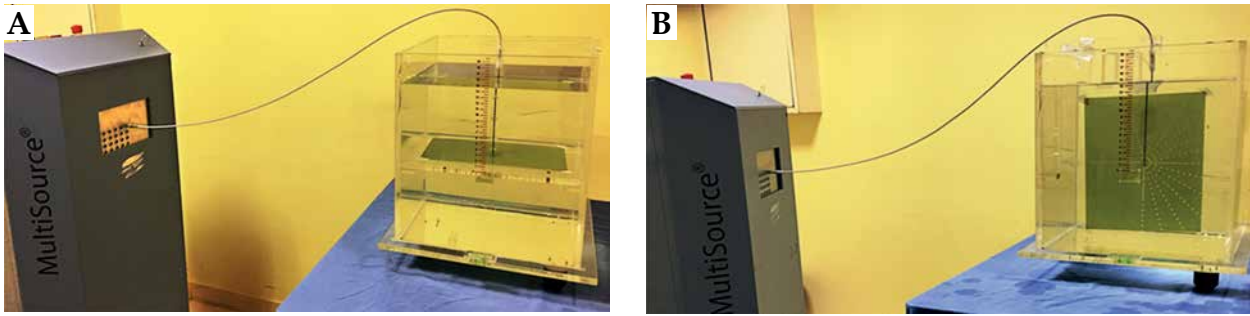


Fig. 3. Experimental setup of specially designed and precisely machined: **(A)** PMMA slab phantom for radial dose function and **(B)** PMMA slab phantom for anisotropy function

tors established in this manner were used to correct the output of each TLD to achieve better precision, of the order of 1% (1σ , type A). The response of the TLD rods per unit dose to water was studied by exposing each group of 5 TLD rods to doses ranging from 10 cGy to 10 Gy in ^{60}Co γ -rays from the Theratron-780C telecobalt unit. The TLDs response with increasing dose was linear up to 10 Gy ($R^2 = 0.999$). The uncertainties in the TLD dose calibration (type B) are found to be 3.5%. The quadrature combined uncertainty for the TLD measurements is 4.2%. All statistical uncertainties on the calculations in the present study have an estimated coverage factor $k = 1$.

Gafchromic EBT2 film

The Gafchromic EBT2 dosimetry film (ISP Technologies) used in this work has a high spatial resolution and is a highly sensitive dosimetry film which can be used in the dose range of 0.01-40 Gy. In comparison to the earlier radiochromic film models, the EBT2 film shows less energy dependency [21]. The EPSON Dual Lens Perfec-

tion V700 desktop scanner was used for scanning the EBT2 films. We followed the film scanning protocol as mentioned by Huet *et al.* [22]. The TIFF images of films were analyzed with the PTW-VeriSoft (version 6.0.1) software. For calibration, the EBT2 film was cut into samples with sizes of $3 \times 3 \text{ cm}^2$ and the orientation of the film was marked at the right corner of each film sample. All the films were irradiated with ^{60}Co γ -rays from the Theratron-780C telecobalt unit for the calibration dose range from 10 cGy to 40 Gy. One sample was left unexposed but kept with the other samples for background optical density. All irradiated films were scanned 24 h after exposure. The net optical density calculation was performed according to published literature [23]. The overall uncertainty calculated using a simple quadrature sum of individual components is found to be 3.8%, which includes type A uncertainty due to scanner consistency of 2% and type B uncertainties of dose conversion from optical density in the calibration procedure in terms of film uniformity and fitted dose value process of 2% and 2.5% respectively.

In-house water phantom and slab inserts

A precisely machined $30 \times 30 \times 30 \text{ cm}^3$ water phantom was designed in-house specifically for the purpose of measuring the radial dose and anisotropy functions. The walls of the phantom were made up of PMMA with 1 cm thickness.

For the measurement of $g(r)$, we fabricated a PMMA slab phantom insert with dimensions of $30 \times 30 \times 1 \text{ cm}^3$, which was carefully machined with an accuracy of 0.1 mm to accommodate the TLD rods and a plastic catheter (2 mm in outer diameter) inside which the source was driven. The holes for the source and the TLD rods were drilled vertically through the plate such that the source centre and the TLD centre were in the same plane. The phantom was designed to have eight TLD rods at each point, from 1 cm to 10 cm, with a suitable design as shown in Figure 2A. The slab containing the TLDs was inserted horizontally in a water phantom and a provision was made to ensure that the PMMA slab containing the TLDs was located at the centre of the phantom, surrounded by the water medium to provide full scattering conditions.

For the measurement of $F(r,\theta)$, another PMMA slab phantom insert of $30 \times 30 \times 1 \text{ cm}^3$ dimensions was fabri-

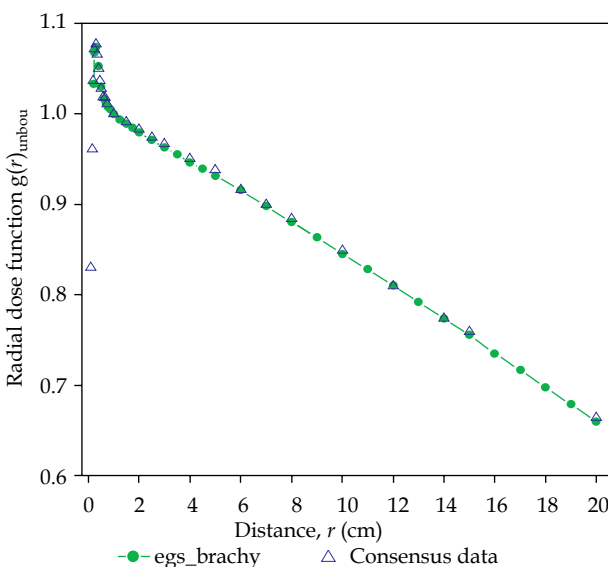


Fig. 4. Comparison of egs_brachy Monte Carlo calculated radial dose function $g(r)_{unbou}$ for BEBIG ^{60}Co source in an unbounded phantom with consensus data. The approximate statistical uncertainty (type A) in our calculation is 0.15%

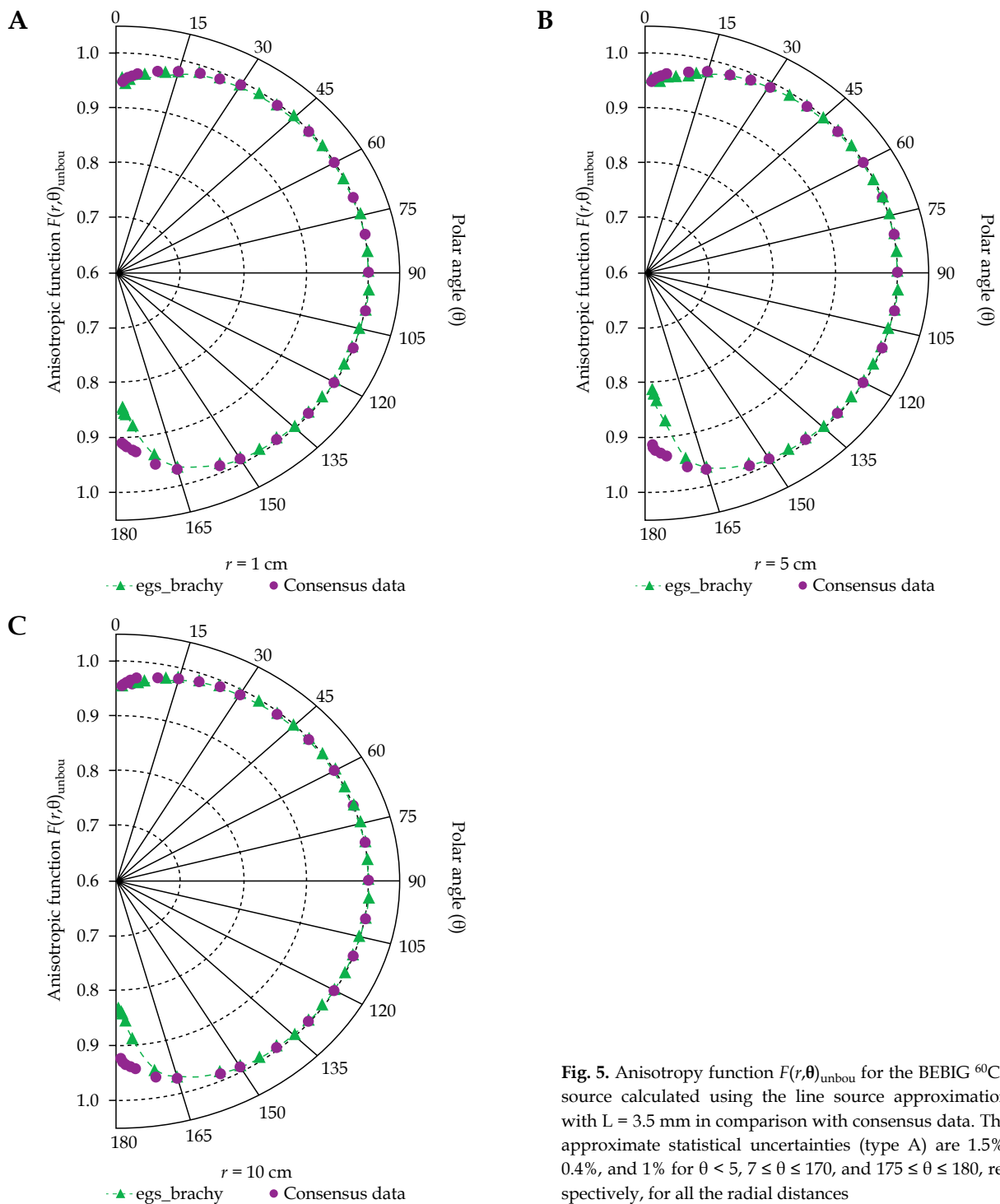


Fig. 5. Anisotropy function $F(r, \theta)_{\text{unbou}}$ for the BEBIG ^{60}Co source calculated using the line source approximation with $L = 3.5$ mm in comparison with consensus data. The approximate statistical uncertainties (type A) are 1.5%, 0.4%, and 1% for $\theta < 5$, $7 \leq \theta \leq 170$, and $175 \leq \theta \leq 180$, respectively, for all the radial distances

cated in which the holes were drilled vertically through the plate to position the TLD rods. The PMMA slab phantom design was as shown in Figure 2B. The design of the PMMA slab was taken from Meigooni *et al.* [24]. The slab containing the TLDs was inserted vertically in a water phantom. The centre of the source was at a depth of 15 cm below water level and at a height of 15 cm from the bottom of the phantom. The EBT2 film measurements were done in the same way as above. The accuracy of the source position in the phantom with respect to the

arrangement of detectors was verified with a square sample of the EBT2 films.

Measurement techniques

TLD-100 method

The TLD measurements of $g(r)$, denoted as $g(r)_{\text{TLD}}$, were performed at distances ranging from 1 cm to 10 cm with 1 cm increments and at angles of 0° , 45° , 90° , 135° , 180° , 225° , 270° , and 315° . The TLD measurements

Table 2. Dose-rate – along-away data in an unbounded liquid water phantom per unit air-kerma strength (cGy h⁻¹ U⁻¹) around BEBIG ⁶⁰Co source

Along (cm)	Away (cm)												
	0.00	0.20	0.40	0.60	0.80	1.00	2.00	3.00	4.00	5.00	10.00	15.00	20.00
-20.0	0.001783	0.001762	0.001757	0.001764	0.001763	0.001761	0.001749	0.001727	0.001696	0.001657	0.00135	0.0009976	0.000698
-15.0	0.003575	0.00358	0.003575	0.003555	0.003547	0.003546	0.003525	0.003461	0.003354	0.003226	0.002363	0.001564	0.001001
-10.0	0.008861	0.008981	0.008964	0.008982	0.00892	0.008977	0.008716	0.008355	0.007843	0.007238	0.004266	0.002374	0.001363
-5.0	0.0392	0.03932	0.03917	0.03908	0.0388	0.03842	0.03484	0.02972	0.02444	0.0198	0.007315	0.003277	0.001689
-4.0	0.06253	0.06197	0.06197	0.06189	0.06098	0.06012	0.05158	0.04106	0.03184	0.02453	0.007956	0.003423	0.00174
-3.0	0.1128	0.1125	0.1119	0.1105	0.1082	0.1048	0.08079	0.0579	0.04125	0.02993	0.008522	0.003548	0.001774
-2.0	0.2574	0.259	0.2538	0.2446	0.2312	0.2148	0.1336	0.08125	0.05203	0.03532	0.008986	0.00364	0.001802
-1.5	0.4692	0.4646	0.4483	0.4163	0.3766	0.3349	0.1722	0.09433	0.05721	0.03775	0.009167	0.003676	0.001814
-1.0	1.093	1.062	0.9574	0.8177	0.6734	0.5509	0.2164	0.1064	0.06162	0.03963	0.009285	0.003698	0.001821
-0.8	1.804	1.668	1.416	1.118	0.8674	0.6731	0.2332	0.1107	0.063	0.04023	0.009324	0.003704	0.001824
-0.6	-	2.973	2.218	1.563	1.11	0.8117	0.2484	0.114	0.06411	0.04061	0.009347	0.003711	0.001823
-0.4	-	6.298	3.644	2.162	1.387	0.9487	0.2603	0.1165	0.06498	0.04101	0.009369	0.003715	0.001826
-0.2	-	15.53	5.705	2.773	1.62	1.056	0.2681	0.118	0.06542	0.04119	0.009362	0.00372	0.001827
0.0	-	23.52	6.878	3.048	1.717	1.098	0.2708	0.1185	0.06552	0.0413	0.00937	0.003724	0.001829
0.2	-	15.63	5.704	2.773	1.623	1.057	0.2683	0.118	0.06543	0.04127	0.009377	0.003719	0.001827
0.4	0.0007772	6.374	3.646	2.162	1.386	0.9484	0.2602	0.1164	0.0649	0.04099	0.009373	0.003719	0.001826
0.6	0.0003125	2.98	2.217	1.563	1.111	0.8108	0.2484	0.1138	0.06412	0.04065	0.009348	0.003709	0.001826
0.8	1.26	1.658	1.414	1.119	0.8657	0.6719	0.2334	0.1105	0.06306	0.04022	0.00931	0.003704	0.001824
1.0	0.9842	1.039	0.9612	0.8195	0.6746	0.5514	0.2161	0.1065	0.06153	0.0396	0.009277	0.003699	0.001823
2.0	0.2237	0.2385	0.2502	0.2441	0.2307	0.2148	0.1335	0.08123	0.05201	0.03527	0.008991	0.003641	0.001803
3.0	0.09734	0.1001	0.1071	0.1085	0.1075	0.1043	0.08094	0.05804	0.04128	0.02989	0.008532	0.003549	0.001777
4.0	0.05354	0.05431	0.05778	0.05955	0.06002	0.05978	0.05151	0.04112	0.03183	0.02451	0.007953	0.003426	0.001735
5.0	0.03324	0.03408	0.03544	0.03705	0.03772	0.03781	0.03483	0.0297	0.02444	0.0198	0.007306	0.003273	0.001689
10.0	0.007769	0.007908	0.007938	0.008104	0.008244	0.008373	0.008617	0.008313	0.007827	0.007238	0.004259	0.002376	0.001364
15.0	0.003202	0.003187	0.003202	0.003223	0.003251	0.003284	0.003404	0.003406	0.003331	0.003216	0.00236	0.001563	0.001003
20.0	0.001626	0.001606	0.001605	0.001618	0.00162	0.001619	0.001668	0.001683	0.001674	0.001641	0.001351	0.0009963	0.0007013

of $F(r,\theta)$, denoted as $F(r,\theta)_{\text{TLD}}$, were performed at radial distances ranging from 1.0 cm to 10 cm in increments of 1.0 cm and at angles of 0°, 15°, 30°, 45°, 60°, 75°, 90°, 105°, 120°, 135°, 150°, and 165°. The TLD data at each point in the phantom were taken from the average of three measurements with a reproducibility of better than 1%. Volume correction factors for the finite size of the TLD rods were calculated by Thomason and Higgins [25]. In this study, we used the published values of this correction factor as 1.028 and 1.0 for distances of 1 cm and beyond 1 cm, respectively. In this work, because the TLDs were calibrated in the ⁶⁰Co beam and exposed to the ⁶⁰Co HDR source, no energy response correction factor was applied.

Gafchromic EBT2 film method

The scanning procedure of irradiated Gafchromic films was kept the same as mentioned above in the film calibration methodology. To obtain $g(r)_{\text{film}}$, the pixel values were noted at radial distances ranging from 1 cm to 10 cm along the perpendicular bisector of the source at angles of 0°, 45°, 90°, 135°, 180°, 225°, 270°, and 315°, for both unirradiated and irradiated films. To calculate the $F(r,\theta)_{\text{film}}$, the pixel values were noted for radial distances ranging from 1.0 cm to 10 cm in increments of 1.0 cm and at angles 0°, 15°, 30°, 45°, 60°, 75°, 90°, 105°, 120°, 135°, 150°, and 165°, for both unirradiated and irradiated films. The energy dependence of the EBT2 film was found to be

relatively small, within measurement uncertainties for all energies and modalities; hence, no correction factor was applied. The experimental setup is as shown in Figure 3.

egs_brachy calculation of $g(r)$ and $F(r,\theta)$ for a bounded phantom

In this study, we mimicked the in-house designed water phantom, with a PMMA boundary of $30 \times 30 \times 30 \text{ cm}^3$ geometry, used in experimental work, as a rectilinear water phantom which includes a 1 cm PMMA plate at the centre of the water phantom for the calculation of $g(r)$ and $F(r,\theta)$, as described in the above sections. For the bounded phantom calculation, we simulated 4×10^9 histories to get 1σ statistical uncertainties (type A) of 2% or less. The voxel sizes were chosen as follows: $0.1 \times 0.1 \times 0.1 \text{ mm}^3$ voxels used for the distance of $r \leq 1 \text{ cm}$, $0.5 \times 0.5 \times 0.5 \text{ mm}^3$ voxels for $1 < r \leq 5 \text{ cm}$ and $1 \times 1 \times 1 \text{ mm}^3$ voxels for $5 < r \leq 10 \text{ cm}$ respectively to provide the adequate spatial resolution. Other than the bounded phantom geometry, all other calculation parameters were kept similar to the unbounded phantom calculation.

Results

Calculated TG43U1 parameters in an unbounded phantom using egs_brachy

The dose rate constant, $\Lambda_{\text{unbou},r}$ for the BEBIG ^{60}Co source is obtained as $1.098 \pm 0.001 \text{ cGyh}^{-1} \text{ U}^{-1}$, whereas the dose rate constant ($_{\text{CON}}\Lambda$) provided by the consensus data was $1.092 \pm 0.011 \text{ cGyh}^{-1} \text{ U}^{-1}$. The radial dose functions, $g(r)_{\text{unbou},r}$ calculated for the line source ($L = 0.35 \text{ cm}$) are shown in Figure 4 from a radial distance of 0.2 cm to 20 cm with corresponding calculated uncertainties of 0.15% (type A), which is in good agreement with the consensus data with maximum deviation of 0.6%. The anisotropy function, $F(r,\theta)_{\text{unbou}}$ for the three radial distances are shown in Figure 5, which is in good agreement, i.e., within 2%, with the consensus data up to $\theta < 175^\circ$, and beyond 175° , a maximum variation of up to 10% is found. The statistical uncertainties (type A) are 1.5%, 0.4%, and 1% for $\theta < 5^\circ$, $7^\circ \leq \theta \leq 170^\circ$, and $175^\circ \leq \theta \leq 180^\circ$, respectively for the radial distance of 0.25 cm to 20 cm. The dose rate around the source is presented as along-away data in Table 2, which is in agreement with the available consensus data within 2%.

egs_brachy calculated and measured $g(r)$ and $F(r,\theta)$ in a bounded phantom

Figure 6 shows the $g(r)$, obtained by the experimental methods, using TLD-100 rods ($g(r)_{\text{TLD}}$) and Gafchromic EBT2 film ($g(r)_{\text{Film}}$), in comparison with the egs_brachy MC calculation, ($g(r)_{\text{bou}}$). The results are shown from 1 cm to 10 cm for both experimental methods, whereas the egs_brachy MC calculated values are shown from 0.2 cm to 10 cm. The variation of the radial dose function, $g(r)$, between the TLD measurement ($g(r)_{\text{TLD}}$) and the egs_brachy MC ($g(r)_{\text{bou}}$), is found to be between 0.2% and 2.4%. In a similar comparison with the EBT2 film measurement ($g(r)_{\text{Film}}$), the variation is found to be between 0.1% and 1.8%. The uncertainties (type A) in the measure-

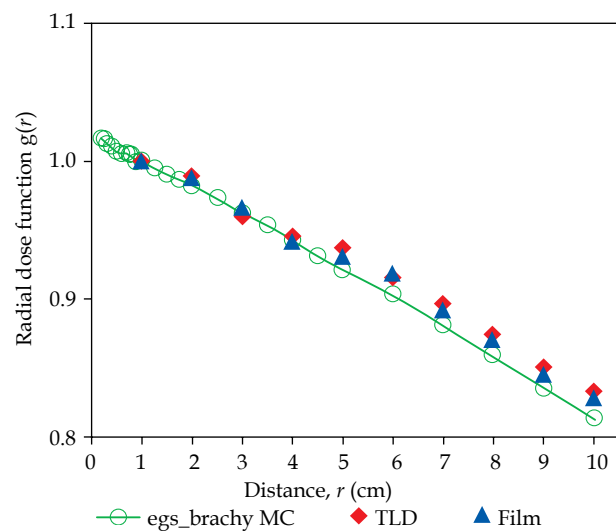


Fig. 6. Comparison between bounded phantom measured radial dose function $g(r)$ using TLD-100 ($g(r)_{\text{TLD}}$), Gafchromic EBT2 Film ($g(r)_{\text{film}}$) and egs_brachy MC calculated ($g(r)_{\text{bou}}$) values. The approximate uncertainties in the measurements (type A) were 1.5% for film, 2% for TLD-100 and 0.5% for egs_brachy calculation

ments were 1.5% for film, 2% for TLD-100 and 0.5% for egs_brachy calculation.

The comparison between the measured $F(r,\theta)$, using TLD-100 ($F(r,\theta)_{\text{TLD}}$) and the Gafchromic EBT2 film, ($F(r,\theta)_{\text{film}}$), with the egs_brachy MC calculated values, ($F(r,\theta)_{\text{bou}}$), for the radial distances of 1, 5, and 10 cm, is shown in Figure 7. The measured values of $F(r,\theta)_{\text{TLD}}$, in comparison with $F(r,\theta)_{\text{bou}}$ show a maximum variation of 2.8% and most of the variations are within 2% for the rest of the points measured. Similarly, a maximum variation of 1.7% is observed in the Gafchromic EBT2 film measurement and most of the measured points vary within 1.5% of the simulation results.

Discussion

As per TG43U1 [2] and HBED Working Group report [3], the MC calculations and their experimental validation methods by any possible dosimeters (e.g., TLD or film) average out the possible biases of each method. After a successful validation, the MC calculated dosimetric parameters can be used as inputs to the clinical dosimetry through treatment planning systems.

It is important to consider the size of the phantom involved when calculating the dosimetric parameters of any brachytherapy dosimetry study, either by the MC calculation or by experimental methods [26,27,28]. Granero *et al.* [9] analyzed the BEBIG ^{60}Co HDR source using the GEANT4 MC code. They provided TG43U1 data such as dose-rate constant, radial dose function, and anisotropy function, and the 2D along and away dose rate table. They used an unbounded liquid water phantom, where the source was immersed in the centre of a spherical water phantom of 50 cm in radius. Guerrero *et al.* [29] used the PENELOPE simulation code for the BEBIG ^{60}Co

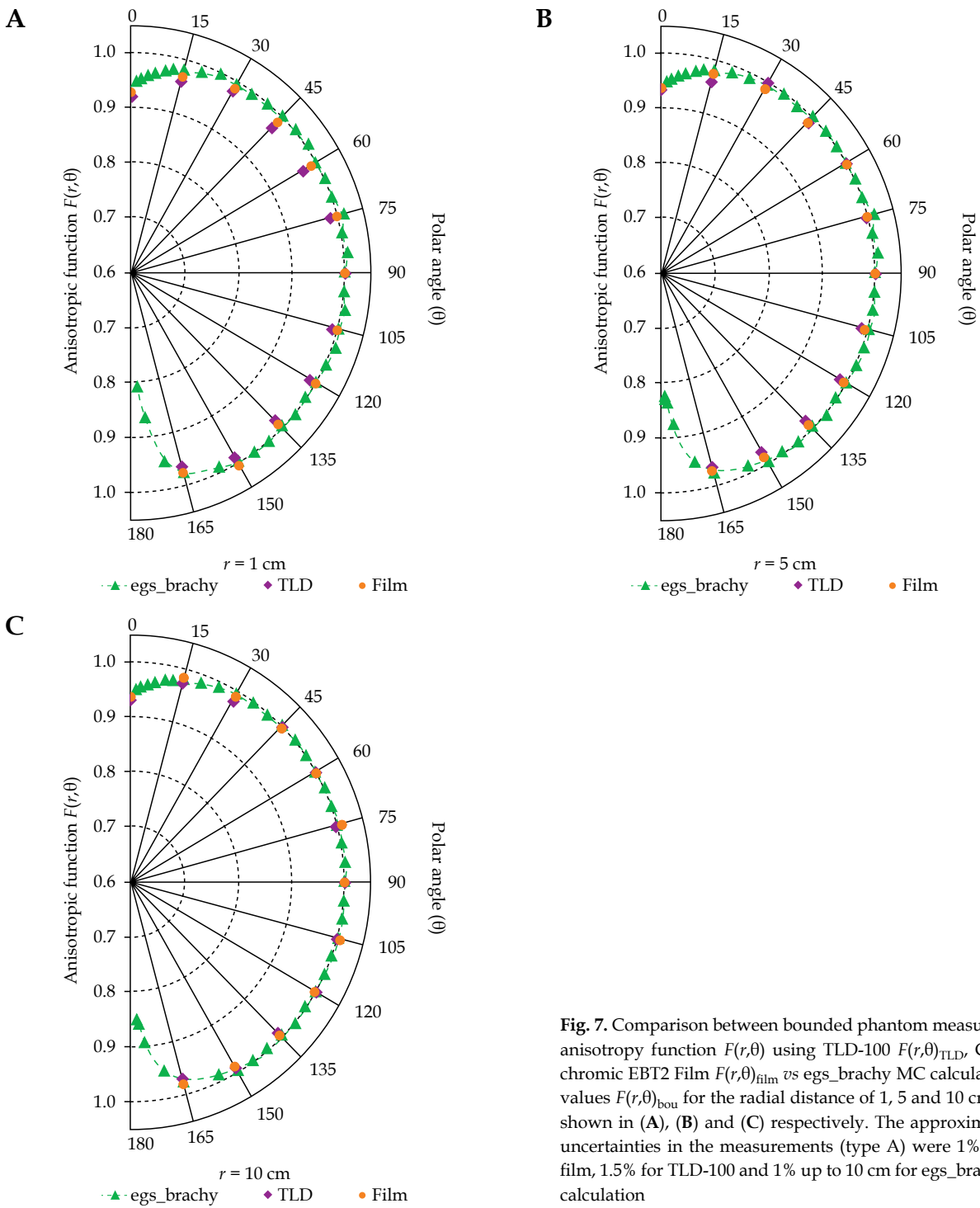


Fig. 7. Comparison between bounded phantom measured anisotropy function $F(r, \theta)$ using TLD-100 $F(r, \theta)_{TLD}$, Gafchromic EBT2 Film $F(r, \theta)_{film}$ vs egs_brachy MC calculated values $F(r, \theta)_{bou}$ for the radial distance of 1, 5 and 10 cm is shown in (A), (B) and (C) respectively. The approximate uncertainties in the measurements (type A) were 1% for film, 1.5% for TLD-100 and 1% up to 10 cm for egs_brachy calculation

HDR source to get a full dosimetric dataset following the guidelines of the AAPM and ESTRO report. All the TG-43 based dosimetric parameters have been calculated for the two different geometries a) Detailed Geometry (G_D) and b) Simplified Geometry (G_S). The main difference between these two is that the conical tip of the source, which is available in G_D , is made to be flat in G_S . Further, the results were compared with other published values of Selvam and Bhola [30], Granero *et al.* [9], and Anwarul *et al.* [31]. According to the results of Guerrero

et al. [29], the $g(r)$, obtained from the G_D and G_S for the BEBIG ^{60}Co HDR source shows a maximum variation of 0.7% between the two different simulated geometries of the source. The relative uncertainties in the $F(r, \theta)$ values were less than 2% in the same study. Selvam *et al.* [30] used an EGSnrc based DOSRZnrc user code which has a limitation of a conical source tip in the modelling, so they used the simplified geometry (G_S) and used a cylindrical water phantom with a length and diameter of 1 m. They compared their results with the GEANT4 based cal-

ulation of Granero *et al.* [9] and found that the dose rate data are higher by 14% along the longitudinal axis where the source cable is connected.

In this study, we calculated the TG43U1 dosimetric dataset for an unbounded liquid water phantom, using the `egs_brachy` application and compared with the consensus data for its validation before comparing its calculation with the measured ($g(r)_{\text{bou}}$) and ($F(r,\theta)_{\text{bou}}$), using TLD-100 and Gafchromic EBT2 film in a bounded phantom.

The comparison of $F(r,\theta)_{\text{unbou}}$ with the consensus data shows a maximum deviation of up to 10% for $\theta \geq 175^\circ$, possibly due to Granero *et al.* [9] having modelled the steel cable length as 1 mm instead of 5 mm, which was discussed by Selvam *et al.* [30] in along-away dose rate differences. From Table 2, it can be seen that the dose rate data along-away table agrees well with the available consensus data. At along $z = 0$ cm and away $y = 0.2$ cm, the value is $23.52 \text{ cGy h}^{-1}\text{U}^{-1}$, which, when compared with the value published by Anwarul *et al.* [31] of $23.2 \text{ cGy h}^{-1}\text{U}^{-1}$, is in agreement, and the variation is 1.4%. Therefore, based on our calculated dosimetric data for the BEBIG ^{60}Co source, using the `egs_brachy` agrees well with the published values.

Subsequent to the validation of the `egs_brachy` calculation, we measured $g(r)$ and $F(r,\theta)$ for the BEBIG ^{60}Co source (Co0.A86) using the TLD-100 and Gafchromic EBT2 film in an in-house water phantom. To compare these experimental results with the MC calculation and to reduce the uncertainty to get more accurate calculation results, we mimicked the geometry of the phantom similar to the experimental setup as a bounded water phantom, because all other published MC results were in an unbounded phantom of radius of either 50 cm or 100 cm, as discussed above. From our results of the $g(r)$ and $F(r,\theta)$, the observed variation between the experimental methods and the `egs_brachy` calculation are found to be well within the acceptable experimental uncertainties of 3%.

Conclusions

In this study, we validated the `egs_brachy` calculation of the TG43U1 dataset for the BEBIG ^{60}Co source for an unbounded geometry. Subsequently, we measured the $g(r)$ and $F(r,\theta)$ for the same source using an in-house water phantom. These parameters are essential for the computation of the dose in the water medium as per the TG43U1 formalism and there are no experimental values in the published literature for the type of source we studied. In addition to this, we validated these experimental results with the values calculated using the `egs_brachy` MC code, with the same geometry and a similar phantom material as used in the experimental methods.

Acknowledgments

The authors would like to thank Prof. Dr. D.W.O. Rogers, CLRP, Carleton University, Canada for his valuable inputs related to MC. The authors are also grateful to Prof. Dr. M.G. Janaki, Head, Radiation Oncology and Mrs. Revathi, Medical Physicist from MSR-Curie Centre of Oncology, Bangalore and Mr. T. VijayaReddy, KMIO

for their support in the experimental work. We extend our sincere thanks to Prof. Dr. S.L. Keshava for his timely help in the discussion part of the manuscript. This work was supported by a UICC International Cancer Technology Transfer Fellowship.

Disclosure

The authors report no conflict of interest.

References

- Li Z, Das RK, DeWerd LA et al. American Association of Physicists in Medicine (AAPM); European Society for Therapeutic Radiology and Oncology (ESTRO). Dosimetric prerequisites for routine clinical use of photon emitting brachytherapy sources with average energy higher than 50 keV. *Med Phys* 2007; 34: 37-40.
- Rivard MJ, Coursey BM, DeWerd LA et al. Update of AAPM Task Group No. 43 Report: A revised AAPM protocol for brachytherapy dose calculations. *Med Phys* 2004; 31: 633-674.
- Perez-Calatayud J, Ballester F, Das RK et al. Dose calculation for photon-emitting brachytherapy sources with average energy higher than 50 keV: report of the AAPM and ESTRO. *Med Phys* 2012; 39: 2904-2929.
- Vijande J, Granero D, Perez-Calatayud J et al. Monte Carlo dosimetric study of the Flexisource Co-60 high dose rate source. *J Contemp Brachytherapy* 2012; 4: 34-44.
- Ballester F, Granero D, Pérez-Calatayud J et al. Monte Carlo dosimetric study of the BEBIG Co-60 HDR source. *Phys Med Biol* 2005; 50: N309-316.
- Pérez-Calatayud J, Ballester F, Serrano-Andrés MA et al. Dosimetry characteristics of the Plus and 12i Gammamed PDR Ir-192 sources. *Med Phys* 2001; 28: 2575-2585.
- Ballester F, Lluch JL, Limami Y et al. A Monte-Carlo investigation of dosimetric characteristics of the CSM11 137Cs source from CIS. *Med Phys* 2000; 27: 2182-2189.
- Sahoo S, Palani Selvam T, Vishwakarma RS et al. Monte Carlo modeling of ^{60}Co HDR brachytherapy source in water and in different solid water phantom materials. *J Med Phys* 2010; 35: 15-22.
- Granero D, Pérez-Calatayud J, Ballester F. Technical note: Dosimetric study of a new Co-60 source used in brachytherapy. *Med Phys* 2007; 34: 3485-3488.
- Taylor REP, Yegin G, Rogers DWO. Benchmarking BrachyDose: voxel-based EGSnrc Monte Carlo calculations of TG-43 dosimetry parameters. *Med Phys* 2007; 34: 445-457.
- Yegin G. A new approach to geometry modelling of Monte Carlo particle transport: an application to EGS. *Nucl Instrum Methods B* 2003; 211: 331-338.
- Kawrakow I, Mainegra-Hing E, Tessier F et al. The EGSnrc C++ class library Technical Report PIRS-898 (rev A) 2009. National Research Council Canada, Ottawa. www.irs.inms.nrc.ca/EGSnrc/PIRS898/
- Chamberland MJP, Taylor REP, Rogers DWO et al. `egs_brachy`: A versatile and fast Monte Carlo code for brachytherapy. *Phys Med Biol* 2016; 61: 8214-8231.
- Taylor RE, Rogers DW. An EGSnrc Monte Carlo-calculated database of TG-43 parameters. *Med Phys* 2008; 35: 4228-4241.
- Taylor REP, Rogers DWO. EGSnrc Monte Carlo calculated dosimetry parameters for ^{192}Ir and ^{169}Yb brachytherapy sources. *Med Phys* 2009; 35: 4933-4934.
- Berger MJ, Hubbell JH. XCOM: photon cross sections on a personal computer. Report NBSIR87-3597, 1987. National Institute of Standards Technology (NIST), Gaithersburg, MD.
- Perkins ST, Cullen DE, Chen MH et al. Tables and Graphs of Atomic Subshell and Relaxation Data Derived from the

- LLNL Evaluated Atomic Data Library (EADL), Z = 1-100. Lawrence Livermore National Laboratory Report UCRL-50400 vol. 30. Lawrence Livermore National Laboratory, Livermore, CA 1991.
18. Kawrakow I, Mainegra-Hing E, Rogers DWO et al. The EGSnrc Code System: Monte Carlo simulation of electron and photon transport. Technical Report PIRS-701, National Research Council Canada 2017.
 19. Walters BRB, Kawrakow I, Rogers DWO. History by history statistical estimators in the BEAM code system. *Med Phys* 2002; 29: 2745-2752.
 20. Booth LF, Johnson TL, Attix FH. Lithium fluoride glow-peak growth due to annealing. *Health Phys* 1972; 23: 137-141.
 21. Bijan A, Ramesh T, Aman A et al. Energy dependence and dose response of Gafchromic EBT2 film over a wide range of photon, electron and proton beam energies. *Med Phys* 2010; 37: 1942-1947.
 22. Huet C, Dagois S, Derreumaux S et al. Characterization and optimization of EBT2 Radiochromic films dosimetry system for precise measurements of output factors in small fields used in radiotherapy. *Radiat Measurements* 2012; 47: 40-49.
 23. Devic S, Seuntjeuns J, Sahm E et al. Precise radiochromic film dosimetry using a flat-bed document scanner. *Med Phys* 2005; 32: 2245-2253.
 24. Meigooni AS, Kleiman MT, Johnson JL et al. Dosimetric characteristics of a new high-intensity ¹⁹²Ir source for remote afterloading. *Med Phys* 1997; 24: 2008-2013.
 25. Thomason C, Higgins P. Radial dose distribution of Ir-192 and Cs-137 seed sources. *Med Phys* 1989; 16: 254-257.
 26. Pérez-Calatayud J, Granero D, Ballester F. Phantom size in brachytherapy source dosimetric studies. *Med Phys* 2004; 31: 2075-2081.
 27. Williamson JF. Comparison of measured and calculated dose rates in water near I-125 and Ir-192 seeds. *Med Phys* 1991; 18: 776-786.
 28. Richter J, Baier K, Flentje M. Comparison of ⁶⁰Cobalt and ¹⁹²Iridium sources in high dose rate afterloading brachytherapy. *Strahlenther Onkol* 2008; 184: 187-192.
 29. Guerrero R, Almansa JF, Torres J et al. Dosimetric characterization of the ⁶⁰Co BEBIG Co0.A86 high dose rate brachytherapy source using PENELOPE. *Phys Med* 2014; 30: 960-967.
 30. Selvam TP, Bhola S. EGSnrc-based dosimetric study of the BEBIG ⁶⁰Co HDR brachytherapy sources. *Med Phys* 2010; 37: 1365-1370.
 31. Anwarul IM, Akramuzzaman MM, Zakaria GA. EGSnrc Monte Carlo-aided dosimetric studies of the new BEBIG ⁶⁰Co HDR brachytherapy source. *J Contemp Brachytherapy* 2013; 5: 148-156.